Proceedings of 14th IOE Graduate Conference
Peer Reviewed
Year: 2023 Month: December Volume: 14
ISSN: 2350-8914 (Online), 2350-8906 (Print)

Flood Hazard Mapping in Ungauged Chandi River Catchment

Raman Shrestha [a], Vishnu Prasad Pandey [b]

[a, b] *Department of Civil Engineering, Pulchowk Campus, IOE, Tribhuvan University, Nepal*
[a] 078mswre011.raman@pcampus.edu.np, [b] vishnu.pandey@pcampus.edu.np

Abstract
This study focuses on preparation of inundation map for the Chandi River Catchment and assessing affected areas across different return periods. Utilizing tools like the Hydrologic Engineering Centre Hydrologic Modelling System (HEC-HMS), Geographic Information System, and Hydrologic Engineering Centre River Analysis System (HEC-RAS), the research incorporates datasets comprising rainfall, discharge data, and Digital Elevation Model (DEM). After the establishment of the HEC-HMS model in the donor catchment, model parameters were obtained, which were then applied to simulate the daily discharge of the Chandi River catchment. Flood discharges for 2-year, 50-year, 100-year, and 1000-year return periods were computed as 133.66 m^3/s, 288.31 m^3/s, 318.85 m^3/s, and 419.77 m^3/s respectively, resulting in inundation area for 2-year, 50-year, 100-year, and 1000-year floods as 1122.9 ha, 1216.5 ha, 1230.8 ha, and 1283.9 ha respectively. Familiar trends were observed in hazard levels, with the percentage under low, moderate, and significant hazard decreasing from 72% in a 2-year flood to 53.3% in a 1000-year flood, and those under extreme hazard increasing from 28% in a 2-year flood to 46.7% in a 1000-year flood with larger return periods. Similarly, the percentage of areas under greater depth increases (2.5% in a 2-year flood and 3.2% in a 1000-year flood for depths exceeding 5 m), while those under lower depth decrease (26.6% in a 2-year flood and 17.2% in a 1000-year flood for depths less than 0.5 m) with an increase in the return period.

Keywords
GIS, HEC-HMS, HEC-RAS, Inundation, Ungauged

1. Introduction

Floods, as defined by the United Nations Office for Disaster Risk Reduction (UNDRR), "is a general and temporary condition of partial or complete inundation of normally dry land areas from overflow of inland or tidal waters, the unusual and rapid accumulation or runoff of surface waters from any source, or the collapse of an alpine snowpack". Due to the quick runoff produced by heavy rainfall, snowmelt, and other contributing variables, flood events can have significant effects in areas with complicated topography and varying climatic conditions, such as the rivers in Nepal [1]. For successful disaster management, land use planning, and infrastructure development in flood-prone locations, accurate flood inundation mapping is crucial [2]. However, it becomes difficult to create accurate flood inundation maps in river basins that are not gauged and where hydrological data is scarce or non-existent [3].

Flash floods and other inundation events frequently occur in the +Chandi River catchment. Due to the unavailability of streamflow data in such areas, conventional hydrological approaches that rely on direct observations of streamflow are frequently insufficient. Therefore, it is necessary to investigate alternate methods that can offer accurate flood inundation information for these ungauged basins [4].

The regionalization method based on the similarity approach is one strategy that has promise. This approach makes use of the notion that hydrological behaviors in many catchments can be similar if they have hydrological and climatic traits in common. It is possible to transfer information from gauged catchments with available data to ungauged ones by detecting and quantifying these commonalities [5]. The regionalization method provides a novel approach to predicting flood characteristics and producing inundation maps for regions where conventional methods fall short [6].

This study focuses on the use of similarity approach for mapping flood inundation in the Chandi River watershed, Nepal. The main goal is to create a solid and adaptable framework that enables flood extent probable inundation pattern prediction in ungauged river basins. This study attempts to fill the data gap and improve our understanding of flood dynamics in the Chandi River basin by leveraging the capabilities of the similarity-based regionalization method.

2. Study Area

The Chandi River catchment is a region of immense ecological and socio-economic importance, but it also carries a history fraught with challenges posed by recurring flooding events. Located within 27°00' to 27°16' N and 85°18' to 85°24' E, this catchment covers an area of approximately 170 km^2. Its hydrological characteristics and land-use patterns make it a unique and critical study area for flood hazard mapping and risk assessment. The Chandi River, originating in the Chure region of Nepal flows through a diverse landscape, encompassing steep mountainous terrain in its upper reaches and gradually transitioning to a flatter and more populated floodplain downstream. The catchment drains into the Bagmati River and plays a pivotal role in the region's hydrology and ecosystem health. The Chandi River catchment has a history scarred by the impacts of flood events. Past occurrences of floods have led to loss of lives, damage to

infrastructure, disruption of agricultural activities, and displacement of communities. These events underscore the urgency of comprehensively mapping flood hazards and implementing effective mitigation measures. The geographical location of the study catchment with its river network is given in Figure 1.

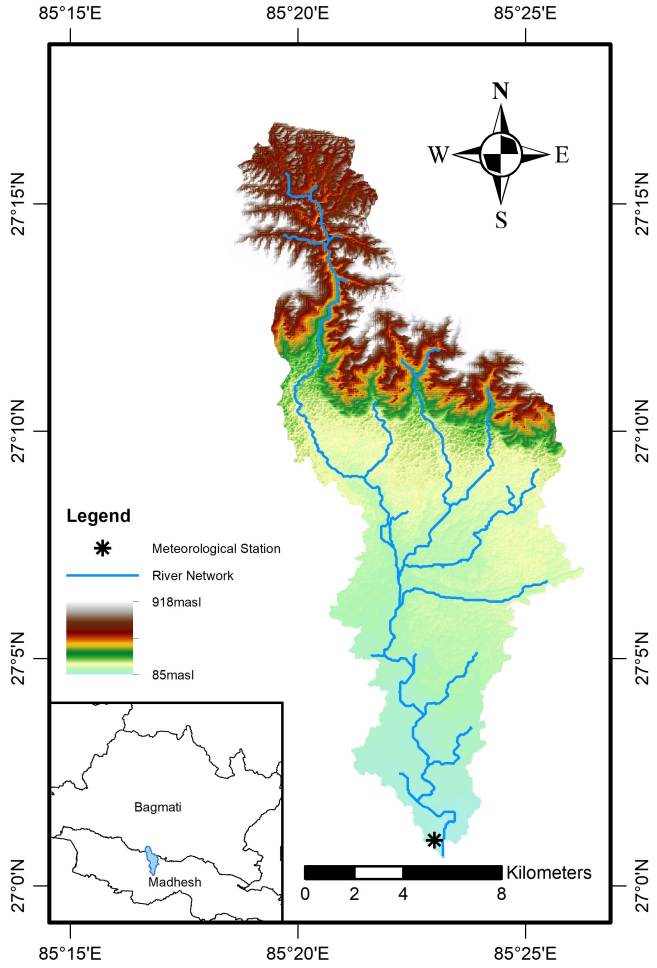

Figure 1: Geographical location of study area

The catchment is entirely located in Rautahat and Makwanpur District. There is no direct national highway access to the site. However, local roads through F07 and F06 can be used to gain access to the site. The elevation of the catchment ranges from 93 masl to 905 masl. More than 50% of the area of the catchment lies in the Terai Region of Nepal. About 65% land is forest area, whereas 0.04% is built-up area according to the Landuse/Landcover (LULC) map of Nepal. There is no discharge gauging station within the station, creating challenges in the validation of the model outputs. However, a precipitation station is located at Ramoli Bariya. The DHM Index of the station is 912. This study relies on the climatic data of DHM Station 912 for the years encompassing the period 1984-2018. Although the amount of precipitation that occurs in the basin fluctuates year by year, on average there is 1675 mm of precipitation throughout the year, as per the records of DHM. The month of June marks the start of precipitation, which lasts until September, just like the typical trend in Nepal.

3. Data and Methods

3.1 Data collection

To determine the donor catchments, various topographic characteristics, climatic characteristics, land use characteristics and soil characteristics are required, which were downloaded from various sources on the internet. Although the data from the web could contain errors, the errors are similar across each catchment and thus the comparative analysis still holds for every donor catchment.

As for hydrological modeling in HEC-HMS, climatic data of precipitation and temperature are required These data are required as input to the model that interacts with the processes in the model to generate the runoff. For the donor, data from the Gaira station (Index:920) from 1987 to 2015 was collected, of which the series from 1987 to 2000, was found to be of adequate quality for hydrological simulation. As for the study catchment, data from the Ramoli Bariya station (Index:912) from 1984 to 2018 was collected.

While simulating floods on rivers with the HEC-RAS software, hydraulic data (flood discharge), computed by flood frequency analysis from the hydrological model output and ALOS PALSA V3 12.5m DEM was used (downloaded from https://search.asf.alaska.edu/).

3.2 Methodology

The study was carried out with the help of the HEC-HMS [7], HEC-RAS [8] and modern techniques in interpretation and analysis based on ArcGIS, as described in Figure 2. The study involves the use of the hydrological model parameters of the donor catchment to the hydrological model setup of the study catchment, to convert the precipitation and temperature input of the study catchment to the discharge on a daily time scale. The daily discharge output of the hydrologic model is then used in the flood frequency analysis to obtain the flood discharge of different return periods. The flood discharge is then used in the hydraulic model to obtain the inundation map of the catchment. The rest of the steps involve the presentation and the interpretation of the results.

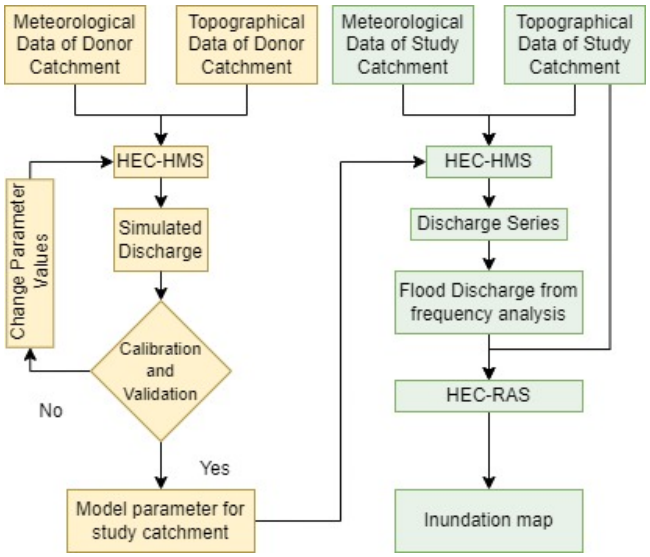

Figure 2: Methodological framework of the study

3.2.1 Hydrologic modelling in HEC-HMS

The HEC-HMS software was applied to convert the rainfall data into discharge data, considering the area of the catchment and the surface characteristics of the modelled location. The processes considered in the model were canopy, surface, loss, transform and baseflow. Simple canopy, simple surface, green and ampt loss, SCS Unit Hydrograph method as transform process and constant monthly baseflow methods were adopted in this study.

For the methods mentioned, the parameters of the similar gauged donor catchments were used, along with the topographical data of the study catchment.

3.2.2 Flood frequency analysis

After the simulation of the daily time series of the study catchment, the yearly peak flow was used in the flood frequency analysis of the catchment. Four different methods (Gumbel's, Extreme Value (EV) 1 Distribution, Log Pearson Type III Distribution and Log normal Distribution) were checked for flood frequency analysis.

Gumbel's Distribution The flood discharge by Gumbel's distribution is computed based on the reduced standard mean and deviation for given sample size. The flood frequency analysis in Gumbel's distribution can be performed using Equation 1 to Equation 3.

$$y_T = -\ln\left[\ln\left(\frac{T}{T-1}\right)\right] \tag{1}$$

$$k = \frac{y_T - \overline{y_n}}{S_n} \tag{2}$$

$$x_T = \bar{x} + K_{\sigma_n} \tag{3}$$

Where, T = Return period, y_n = Reduced mean for corresponding number of data, S_n = Reduced standard deviation for corresponding data, X_t = Flood discharge of return period T, Mean(x) = Average annual peak discharge and σ_n = Standard deviation of the annual peaks

Extreme Value (EV) 1 distribution EV1 Distribution is a quite simple method, that uses just the annual peak and the return period for discharge computation (Equation 4).

$$x_T = \bar{x} - \frac{\sqrt{6}}{\pi}\left[0.5772 + \ln\left\{\ln\left(\frac{T}{T-1}\right)\right\}\right] \tag{4}$$

Where, X_T = Flood discharge of "T" return period and $\bar{x}$ = Mean of annual peak discharge.

Log Pearson Type III distribution Log Pearson Type III distribution computes flood discharge on the basis of coefficient of skewness, and the logarithm of the annual peak values (Equation 5 to Equation 7).

$$C_s = \frac{N\Sigma(Z-\bar{Z})^3}{(N-1)(N-2){\sigma_Z}^3} \tag{5}$$

$$Z_T = \bar{Z} + K_T\sigma_z \tag{6}$$

$$x_T = 10^{Z_T} \tag{7}$$

Where, C_s = Coefficient of skewness, Z = Logarithm of peak annual discharge, $\bar{Z}$ = Average of Z, σ_Z = Standard deviation of Z series, K_T can be obtained from table and X_T = Flood discharge of "T" return period.

Log normal distribution The Log normal distribution is similar to the Log Pearson Type III. The only difference is the that Coefficient of skewness is taken as zero in this approach.

3.2.3 Hydraulic modelling in HEC-RAS

The one-dimensional HEC-RAS model was setup using the 12.5 m DEM of the study area. Using the HEC-GeoRAS extension in ArcGIS, the centerline, bank line, flow lines and cross sections were created. The cross-sections were spaced at an interval of 200 m. However, additional cross sections were created in the curves to capture the actual geometry of the river, as far as possible. Equation 8 and Equation 9 are the general equations used in HEC-RAS.

$$Z_2 + Y_2 + \frac{a_2 V_2^2}{2g} = Z_1 + Y_1 + \frac{a_1 V_1^2}{2g} + h_e \tag{8}$$

$$h_e = Ls_f + C\left|\frac{a_2 V_2^2}{2g} - \frac{a_1 V_1^2}{2g}\right| \tag{9}$$

Where, L = Discharge weighted reach length, S_f = Depresentative friction slope between two sections and C = expansion or contraction loss coefficient

3.2.4 Hazard rating

The depth and velocity output of HEC-RAS were used to prepare the hazard map of the study catchment. For this purpose, the relation that uses depth, velocity and debris factor was used [9].

$$HR = DF + d(v + 0.5) \tag{10}$$

where, d = Depth of inundation , v = Velocity of flow and DF = Debris factor, considered on the assumption that debris also causes significant damage.

The hazard was then classified. The classification is based on the thresholds above which people cannot stand in floodwater due to either being knocked off balance by the speed of the flow and/or becoming buoyant in deeper water [9].

Table 1: Flood hazard rating [9]

S.N	HR (m^2/s)	Rating	Description
1	0 - 0.75	Low	Caution
2	0.75 - 1.5	Moderate	Dangerous for children
3	1.5 - 2.5	Significant	Dangerous for most
4	2.5+	High	Dangerous for all

4. Results

4.1 Hydrological Model Performance in Donor Catchment

Figure 3 and Figure 4 depict the hydrograph pattern of observed and simulated streamflow, respectively. The rainfall-runoff model performed well for the donor catchment, as evidenced by the Nash-Sutcliffe Efficiency (NSE) values of 0.61 and 0.59 during the calibration and validation periods, respectively. The coefficient of determination (R^2) also exhibited satisfactory values of 0.62 and 0.63 for calibration and validation, respectively. Additionally, the Percent Bias (PBIAS) fell within an acceptable range, with values of -13.24% and -7.51% during the calibration and validation periods, respectively. respectively and the Root Mean Square Error (RMSE) values for calibration and validation were 11.79 and 9.09 respectively. Although these values are not in the appropriate ranges, the model is satisfactory from the visual inspection of the time series and Flow Duration Curve (FDC).

Although these values are not particularly great for a simulation, the discharge required for our study had good statistical parameters. For the computation of the flood discharge, annual maximum discharge is used and for annual maximum discharge, NSE, R^2, PBIAS and RMSE were obtained as 0.79,0.87,5.92,46.24 respectively for calibration period and 0.75, 0.82, 8.13% and 42.11 respectively for validation period and these values are a result of good model simulation. So, the parameter of the simulation was found very good to represent the peak flow and good to represent the daily flows.

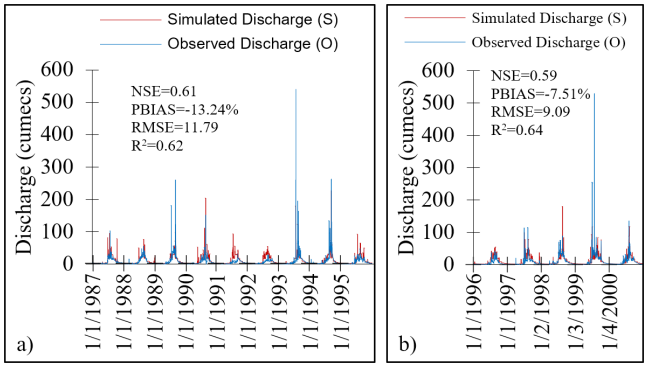

Figure 3: Modelled and observed discharge in a) Calibration and b) Validation

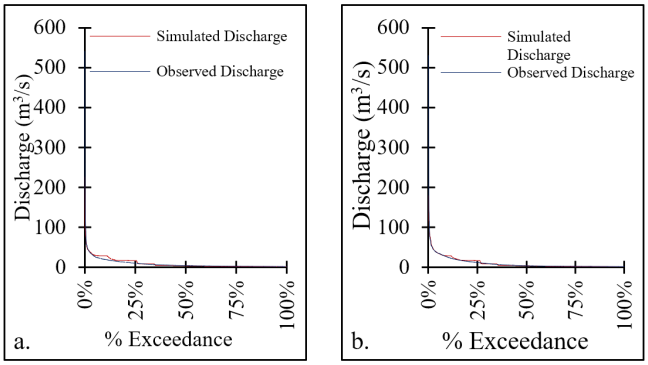

Figure 4: FDC in a)calibration and b)validation in donor catchment

4.2 Peak Discharge Computation

Peak discharge is an essential input parameter in the hydraulic modelling in the HEC-RAS model, as this input drives the hydraulic model into calculating the depth and velocity at the various sections. Using the four distributions, the flood frequency analysis was performed, to calculate the discharge values of various return periods (Figure 5). From the frequency analysis, the peak discharge, computed by Gumbel's distribution method was used. This is because, as the inundation mapping depends on the extreme values and as the data availability is limited, Gumbel's distribution is the preferred choice. On top of that, the yearly maximum daily discharge of the catchment followed the Gumbel distribution, as per several tests performed.

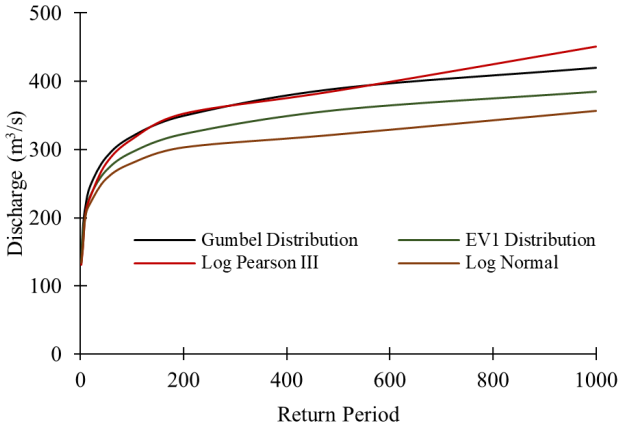

Figure 5: Flood Frequency Analysis

The 2-year, 50-year, 100-year and 1000-year floods were computed as 133.66 m^3/s, 288.31 m^3/s, 318.85 m^3/s and 419.77 m^3/s respectively.

4.3 Performance of HEC-RAS Model

The results of the HEC-RAS model were compared with the depth of inundation, surveyed at four different locations in the site. Two flooding events were considered. The return period analysis of the rainfall of these two events revealed that these events were 2-year and 5-year floods. The manning's constant, initially taken from literature for land use categories was changed, slightly until the surveyed and the modeled depth at these four locations were close enough (NSE value of 0.879, KGE value of 0.758, R^2 value of 0.99 and RMSE of 0.22 m). The optimized Manning's value was used in another flood event and the performance parameters were found satisfactory in the second event as well (NSE = 0.825, KGE =

Table 2: Simulated and surveyed depth at selected points

S.N	Event 1 Modelled Depth (m)	Event 1 Surveyed Depth (m)	Event 2 Modelled Depth (m)	Event 2 Surveyed Depth (m)
1	0.98	0.81	0.95	0.78
2	1.84	1.50	1.75	1.32
3	0.27	0.29	0.21	0.25
4	1.65	1.45	1.60	1.39

0.702, R^2 value of 0.98 and RMSE of 0.255 m). The details of the depth in these four locations are presented in Table 2. These values suggest that the hydraulic model performance for the study catchment was very good. Then, the results of the model were used for further analysis and interpretation.

4.4 Spatial Distribution of Flood

After calibrating Manning's constant with respect to the two floods, the flood inundation map of the catchment for the four different return periods; 2-year, 50-year, 100-year and 1000-year were prepared.

The flood hazard maps of the four selected return periods were prepared by the the raster calculator and reclassify tools in the ArcGIS environment and are presented in Figure 6. It can be observed that the area of high flood hazard is concentrated in the periphery of the river channel, apart from the area in the southern part of the catchment, just south of the settlement near Chapur, which is one of the major settlements of the catchment. Thus, flood adaptation measures, like flood plain management, early warning systems, financial and non-financial risk sharing between communities and individuals will play a huge role in dealing with the potential floods, in these areas.

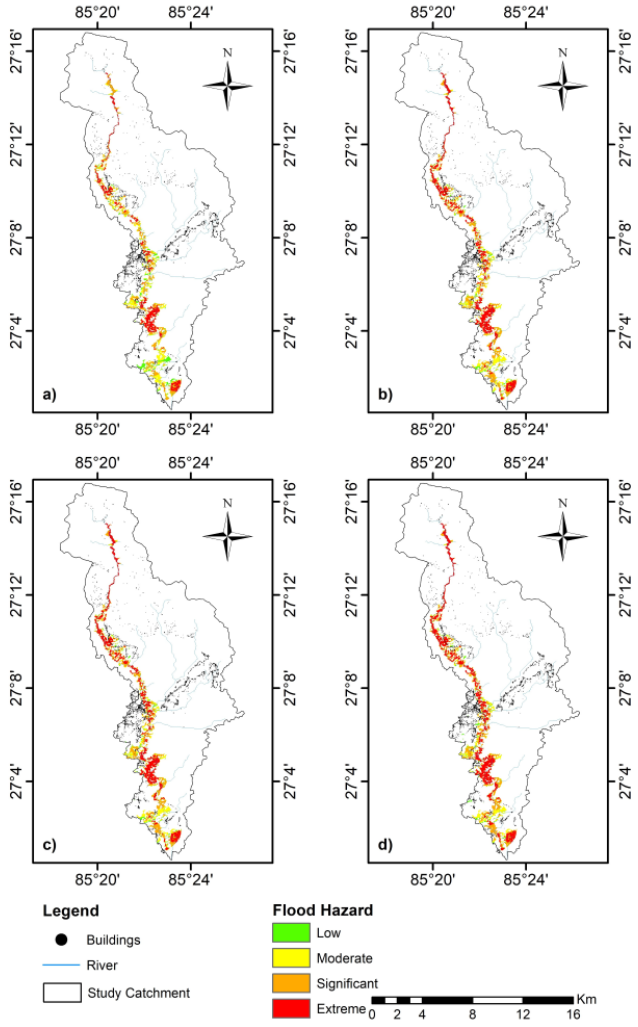

Figure 6: Flood hazard classification for a)2, b)50, c)100 and d)1000 year flood

The total area inundated by these floods of the selected return period is shown in Table 3. The total area inundated increases with longer return periods, indicating a higher flood risk associated with infrequent but more severe events. Specifically, for a 2-year return period, the inundated area is hectares. In the case of a 50-year return period, the inundated area expands to 1216.5 hectares. For a 100-year return period, the area further increases to 1230.8 hectares and in the event of a rare 1000-year return period flood, the area reaches its peak at 1283.9 hectares.

Table 3: Total area inundated for different return period

S.N	Return Period	Area (ha)
1	2-year	1122.9
2	50-year	1216.5
3	100-year	1230.8
4	1000-year	1283.9

All of the inundated areas, however, do not fall under the same hazard category. As per the classification given in Table 1, the hazard has been classified into four different categories. The trend of area proportion under these different hazard categories with respect to different return periods is presented in Figure 7. The data associated with the figure is presented in Table 4. The results demonstrate the changing hazard levels associated with different return periods. For a 2-year return period, the majority of the inundated area falls within the Moderate (24.9%) and Significant (34.5%) categories, with lower proportions in the Low (12.6%) and Extreme (28.0%) categories. As the return period increases to 50 years, the Extreme category sees a significant rise to 40.0%, indicating a heightened risk for severe flooding events. The 100-year return period shows a similar trend, with the Extreme category dominating at 41.7% and in the rare event of a 1000-year return period flood, the Extreme category accounts for a substantial 46.7% of the inundated area.

From Figure 7 and Table 4, it can be observed that as the return period lengthens, the proportion of the extreme hazard significantly increases. This indicates that the risk of experiencing extremely severe flooding events becomes more pronounced with longer return periods. In essence, the table highlights the heightened vulnerability to catastrophic flooding as we move from shorter return periods to rarer, more extreme events.

Table 4: Percentage area under different hazard category with respect to return period

Return Period	Low	Moderate	Significant	Extreme
2	12.6%	24.9 %	34.5 %	28.0 %
50	7.5%	19.7 %	32.8 %	40.0 %
100	7.1%	19.2 %	32.0 %	41.7 %
1000	6.7%	16.7 %	29.9 %	46.7 %

This necessitates the incorporation of long-term flood hazard assessments into disaster planning and management. Although the frequency of extreme events may be relatively

low, their impact can be devastating, strategies and infrastructure should be designed to withstand and respond effectively to such rare but highly destructive flooding scenarios.

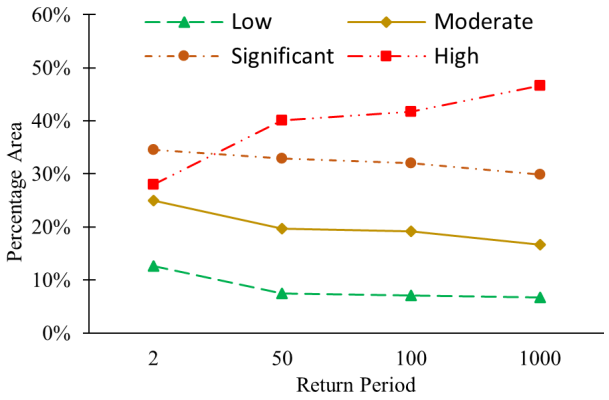

Figure 7: Trend of area proportion of different hazard category with return period

The inundation has also been analyzed based on the depth of the flood. Five different classifications of the depths (<0.5m, 0.5-1.0m, 1.0m-2.0m, 2.0m-5.0m and >5.0m) have been analyzed. The depth map of these categories for the selected return periods is presented in Figure 8.

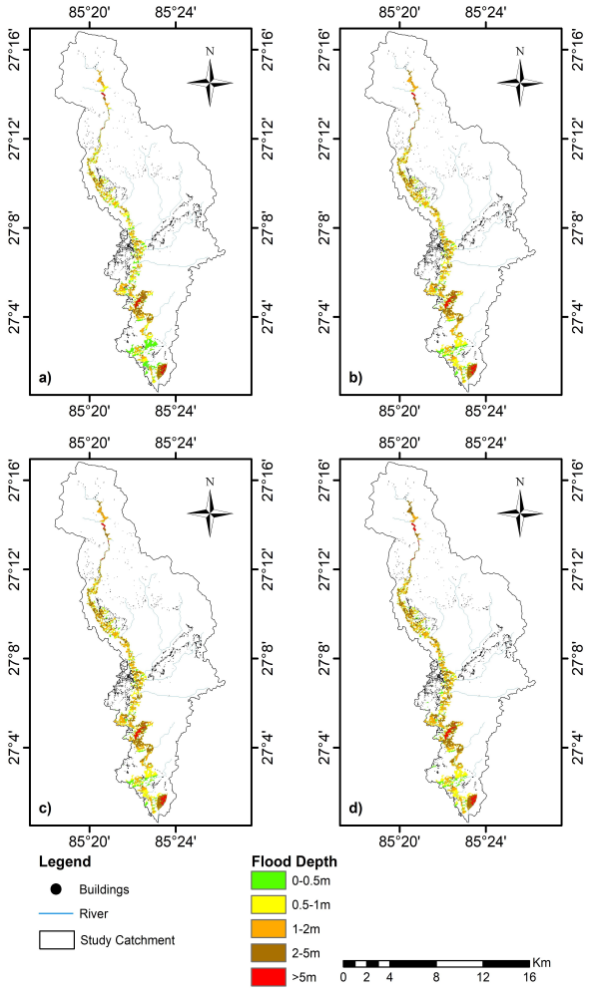

Figure 8: Flood depth classification for a)2, b)50, c)100 and d)1000 year flood

From Figure 8, it can be observed that the area of maximum depth is concentrated in the upper reaches of the river, the settlement near Ramoli Bariya and the southern part of the river. This spatial distribution is similar in all four return periods. The only difference is that with the increase in return period, the total inundated area is expected to increase, but the spatial distribution of the depth is expected to follow the same pattern.

Similarly. the trend of area proportion under these depth classifications with respect to the return period is presented in Figure 9. The data associated with the chart is presented in Table 5.

Figure 9 and Table 5 present an analysis of the percentage area inundated under various depth categories for different return periods, shedding light on the spatial distribution of flooding depths. The results reveal significant insights into the relationship between return periods and inundation depths, offering crucial information for flood risk assessment and disaster management.

Table 5: Percentage area under different depth category with respect to return period

Return Period	<0.5m	0.5-1.0m	1-2m	2-5m	>5m
2	26.6%	22.0 %	29.9 %	19.0 %	2.5 %
50	18.7%	23.2 %	32.4 %	22.9 %	2.8 %
100	18.1%	22.9 %	32.6 %	23.6 %	2.9 %
1000	17.2%	21.6 %	32.0 %	23.6 %	3.2 %

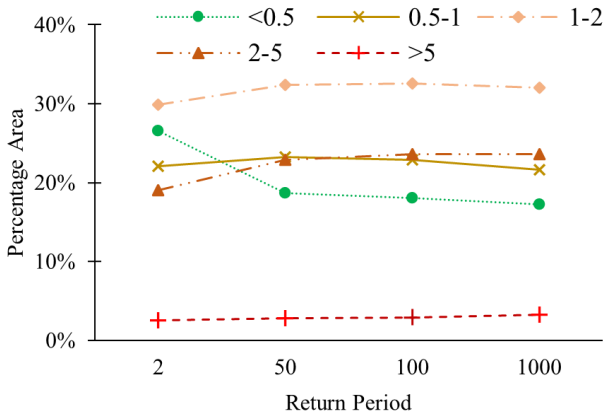

Figure 9: Trend of area proportion of different depth category with return period

For a 2-year return period, the table illustrates that the majority of the inundated area is characterized by depths between 1.0 and 2.0 meters, accounting for 29.9% of the total area. This is followed by areas with depths less than 0.5 meters (26.6%) and depths between 0.5 and 1.0 meters (22.0%). It is evident that, for this return period, shallow flooding (<0.5m) and moderate depths (1.0-2.0m) dominate the inundated landscape.

As the return period extends to 50 years, a clear trend emerges. The percentage areas experiencing deeper flooding (1.0-2.0m and 2-5m) notably increases to 32.4% and 22.9%, respectively. This indicates that longer return periods are associated with a

higher likelihood of more substantial inundation depths. The analysis for a 100-year return period reinforces this trend, with a continued rise in the percentage areas experiencing deeper flooding depths, particularly in the "1.0-2m" (32.6%) and "2-5m" (23.6%) categories. In the event of an extremely rare 1000-year return period flood, the trend persists. A significant portion of the area experiences depths between 1.0 and 2.0 meters (32.0%), and the proportion of areas with depths exceeding 2.0 meters increases to 26.8%.

It was observed that there is a distinct correlation between return periods and the depth of inundation. Longer return periods are consistently associated with a higher likelihood of more extensive and deeper flooding. This observation has profound implications for flood risk assessment and disaster preparedness.

In practical terms, it suggests that communities and authorities must be well-prepared for rare, high-return-period flood events that have the potential to cause more significant damage due to deeper flooding depths. Infrastructure planning, evacuation procedures, and floodplain management strategies should be designed to address the increasing depth of inundation associated with these infrequent but severe flood occurrences.

Furthermore, it emphasizes the necessity of proactive measures, such as improved early warning systems and comprehensive floodplain management, to reduce the potential consequences of extreme flooding events.

5. Conclusions

This research has successfully implemented a methodology for flood hazard mapping in the ungauged Chandi river catchment. Leveraging data from a similar donor catchment, hydrological model parameters were computed, applicable for the ungauged catchment. Applying these parameters to the study catchment, the daily discharge of the study catchment was simulated, resulting in a peak discharge of 133.6 m^3/s, 288.31 m^3/s, 318.85 m^3/s and 419.77 m^3/s for during a 2-year, 50-year, 100-year and 1000-year flood respectively. These values were then used in HEC-RAS to generate velocity and depth maps of the catchment.

- The portion of the catchment close to the river has a larger inundation depth. The total area inundated increases substantially with longer return periods (1122.9 m^2, 1216.5 m^2, 1230.8 m^2 and 1283.9 m^2 during a 2-year, 50-year, 100-year and 1000-year flood respectively), highlighting the heightened risk associated with less frequent but more severe flooding events.
- Inundated areas in the catchment exhibit a consistent decrease in percentage under shallower depths and an increase in those under greater depths with increasing return periods. Notably, areas with depths less than 0.5 meters decrease from 26.6% in a 2-year flood to 17.2% in a 1000-year flood, while areas with depths greater than 5 meters increase from 2.5% to 3.2% over the same period.
- Similar to the trend of depth, the inundated area under low, moderate and significant hazard classification decreased and that under extreme hazard classification increased with return period. The total area under low, moderate and significant hazard decreased from 72% in 2-year flood to 53.3% in 1000-year flood and the area under extreme hazard increased from 28% in 2-year flood to 46.7% in1000-year flood.

Acknowledgments

The authors are thankful to the Department of Hydrology and Meteorology for providing the necessary data and Pulchowk Campus for the good working environment.

References

[1] Landell Mills. Nepal: Flood risk sector assessment consultant report, asian development bank, 2019.

[2] Buddhi Raj Shrestha, Liladhar Sapkota, and Chhabi Lal Chidi. Flood risk mapping and analysis: A case study of andheri khola catchment, sindhuli district, nepal. 2022.

[3] Rofiat Bunmi Mudashiru, Nuridah Sabtu, Ismail Abustan, and Waheed Balogun. Flood hazard mapping methods: A review. *Journal of hydrology*, 603:126846, 2021.

[4] Shuang Liu, Zhenghui Xie, Yujin Zeng, et al. Discharge estimation for an ungauged inland river in an arid area related to anthropogenic activities: A case study of heihe river basin, northwestern china. *Advances in Meteorology*, 2016, 2016.

[5] Richard Arsenault, Mélissa Breton-Dufour, Annie Poulin, Gabrielle Dallaire, and Rabindranarth Romero-Lopez. Streamflow prediction in ungauged basins: analysis of regionalization methods in a hydrologically heterogeneous region of mexico. *Hydrological Sciences Journal*, 64(11):1297–1311, 2019.

[6] Teemu S Kokkonen, Anthony J Jakeman, Peter C Young, and Harri J Koivusalo. Predicting daily flows in ungauged catchments: model regionalization from catchment descriptors at the coweeta hydrologic laboratory, north carolina. *Hydrological processes*, 17(11):2219–2238, 2003.

[7] William A. Scharffenberg. *Hydrologic Modeling System HEC-HMS User's Manual*, 2013.

[8] Gary W. Brunner. *HEC-RAS River Analysis System Hydraulic Reference Manual*, 2016.

[9] Steven Wade, David Ramsbottom, Peter Floyd, Edmund Penning-Rowsell, and Suresh Surendran. Risks to people: developing new approaches for flood hazard and vulnerability mapping. 2005.